International Geology Review, Vol. 48, 2006, p. 882–891.

Zircon-Inclusion Mineralogy of a Diamond-Grade Eclogite from the Kokchetav Massif, Northern Kazakhstan

KAZUAKI OKAMOTO,[1]

Institute of Earth Sciences, Academia Sinica, P.O. Box 1-55 Nankang, Taipei 115, Taiwan ROC

IKUO KATAYAMA,

Geology and Geophysics, Yale University, 210 Whitney Avenue, New Haven, Connecticut 06520

SHIGENORI MARUYAMA,

Department of Earth and Planetary Sciences, Tokyo Institute of Technology, Ookayama, Meguroku, Tokyo 152-8551, Japan

AND J. G. LIOU

Department of Geological and Environmental Sciences, Stanford University, California 94305

Abstract

In order to understand the dehydration process related to phengite decomposition during subduction of crust into the deep mantle, we systematically investigated mineral inclusions in zircons from Kokchetav diamond-grade eclogites. In the eclogites, phengite is absent from the matrix but only occurs as inclusions in clinopyroxene. The clinopyroxene is zoned; the core augite contains K_2O up to 0.24 wt%, whereas the rim omphacite contains secondary K-feldspar inclusions. Phengite may have been consumed during prograde reactions, and K was fixed in clinopyroxene or in a fluid/melt phase. Inclusions of clinopyroxene and garnet were identified in zircon cores, whereas garnet, rutile, quartz, and composite inclusions are present in the mantles and quartz occurs in the rims. Distribution of mineral inclusions in zoned zircons indicates that zircon cores grew at the peak UHP stage, whereas the rims grew in the quartz stability field during decompression. The composite inclusions have assemblages of albite + glass + epidote, rutile + ilmenite, quartz + rutile, and rutile + albite. The former three-phase composite inclusions have rounded outlines and triple-junction grain boundaries, suggesting crystallization from fluid or melt. During the growth of zircon from core to mantle, phengite was consumed, and new garnet, rutile and fluid/melt were formed.

Introduction

THE ORIGIN OF island-arc volcanism is closely related to the dehydration of subducting lithosphere (e.g., Tatsumi et al. 1986; Tatsumi and Eggins, 1995). In the case of cold subducting oceanic crust, most of the fluids are released at depths < 75 km due to dehydration of amphibole. However, lawsonite can still carry a considerable amount of fluid at depths up to 300 km beneath the volcanic front (Poli and Schmidt, 1995; Schmidt and Poli, 1998; Okamoto and Maruyama, 1999; Peacock and Wang, 1999; Usui et al., 2003). In the case of warm subduction of oceanic crust, phengite is the only hydrous mineral stable at depths from 100 to 300 km (Schmidt, 1996, Schmidt et al., 2004; Okamoto and Maruyama, 1998). Study of dehydration processes of the oceanic lithosphere related to phengite decomposition is important in order to understand the origin of back-arc volcanism, inasmuch as back-arc volcanics contain higher K_2O contents resulting from dewatering of subducting lithosphere at greater depths (150–170 km) (e.g., Tatsumi and Eggins, 1995).

Diamond-grade ultrahigh-P (UHP) eclogite from the Kumdy-Kol region of the Kokchetav Massif, northern Kazakhstan, is the best natural sample to investigate the phengite-dehydration process, because the UHP metamorphism occurred at phengite-terminal P-T conditions (>5 GPa, 1000°C) (Okamoto et al., 2000; Fig. 1). In fact, mineral assemblages of Kumdy-Kol eclogites do not contain phengite in the matrix; this phase is only preserved in the core of high-K augite (0.24 wt%) (Table 2 and Fig. 12 of Okamoto et al., 2000). That is, phengite was consumed during prograde (or early retrograde)

[1]Corresponding author; email: kazu@earth.sinica.edu.tw

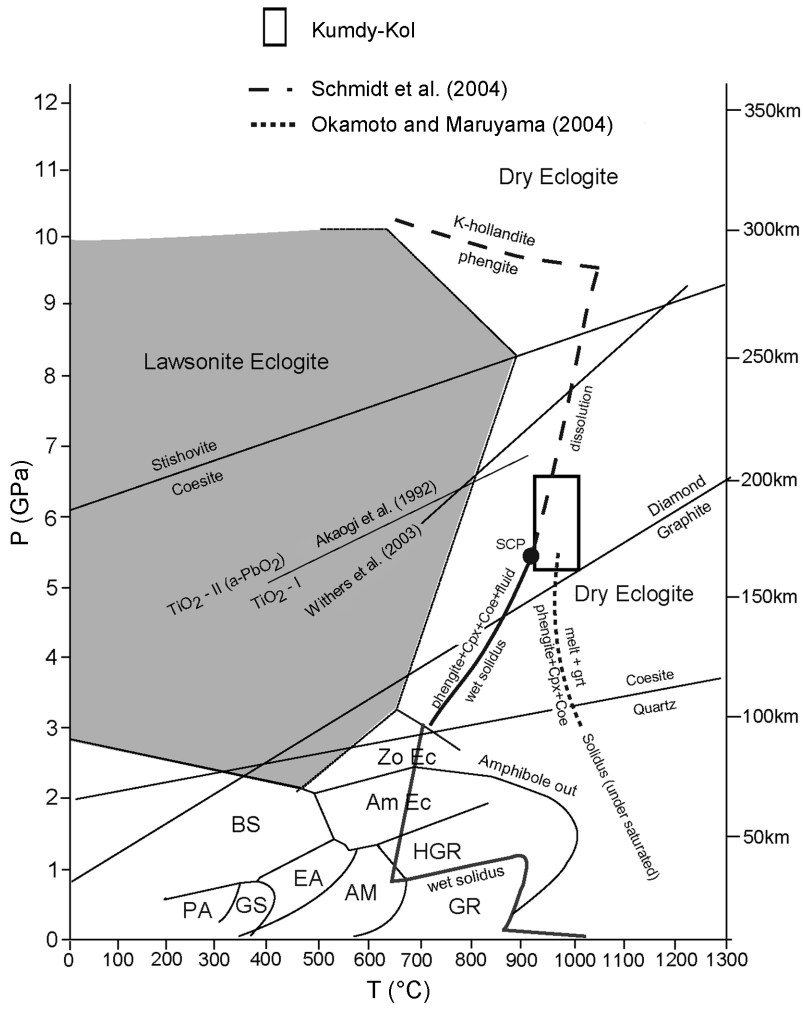

FIG. 1. Phase diagram for the MORB +H_2O system showing the P-T condition of the Kumdy-Kol eclogite (modified from Okamoto et al., 2000). Abbreviations: PA = pumpellyite-actinolite facies; GS = greenschist facies; EA = epidote-amphibolite facies; AM = amphibolite facies; GR = granulite facies; HGR = high-pressure granulite facies; BS = blueschist facies; Grt = garnet; Cpx = clinopyroxene; coe = coesite; SCP = second critical point. The quartz-coesite curve is adapted from Bohlen and Boettcher (1982). Diamond-graphite curve is adapted from Bundy (1980). TiO_2 II (α-PbO_2) – TiO_2 I is adapted from Akaogi et al. (1992) and Withers et al. (2003). The other index reaction curves are adapted from Poli and Schmidt (1995), Maruyama et al. (1996), and Okamoto and Maruyama (1999).

reactions and K might have been transported to the mantle wedge above the subduction slab with fluid or melt. However, detailed evidence was obliterated by extensive symplectization during late-stage amphibolite-facies overprinting related to exhumation.

Zircon is the best UHP metamorphic mineral container due to its extreme resistance and stability over a large pressure-temperature range of conditions (e.g., Chopin and Sobolev, 1995). The study of mineral inclusions in zircon separates from Kokchetav UHP rocks has documented several significant discoveries (e.g., Sobolev and Shatsky, 1990; Katayama et al., 2000a, 2000b, 2002). In order to understand the dehydration process related to phengite decomposition, we investigated mineral

TABLE 1. Mineral Parageneses in Matrix, Clinopyroxene, and Zircon[1]

Sample	Grt	Cpx	Qtz	Rut	Ilm	Ab	K-fel	Phn	Epi	Gl	Comp.[2]
Matrix	+	+	+	+							
Symplectite		+			+	+					
Inclusion in cpx							+				
Inclusion in zircon											
Zircon core	+	+									
Zircon mantle	+			+						+	+
Zircon rims	+		+	+							
Composite inclusions											
Pl + Epi + Gl						+			+	+	
Grt + Rut	+			+							
Ab + Rut				+		+					
Qtz + Rut			+	+							
Rut + Ilm				+	+						

[1]Mineral abbreviations: Grt = garnet; Cpx = clinopyroxene; Qtz = quartz; Rut = rutile; Ilm = ilmenite; Ab = albite; K-fel = K alkali-feldspar; Phn = phengite; Epi = epidote; Gl = glass.
[2]Composite inclusions.

inclusions in zircons of a diamond-grade eclogite from Kumdy-Kol.

Geological Setting

The Kokchetav Massif is situated in the central domain of the composite Eurasian craton, and underwent Cambrian collisional orogenic events (Dobretsov et al., 1995). This massif is composed of several Precambrian rock series, Cambro-Ordovician volcanic and sedimentary rocks, Devonian volcanic molasse, and Carboniferous-Triassic shallow-water and lacustrine sediments; these rocks were intruded by multi-stage granitoids (Dobrestov et al., 1995). The UHP-HP metamorphic unit of the massif is a thin (1–2 km), more or less coherent, subhorizontal sheet, structurally overlain by a weakly metamorphosed unit, and underlain by the Daulet Suite (Kaneko et al., 2000). The UHP-HP unit mainly consists of para- and orthogneiss, marble, eclogite, and amphibolite. Eclogites occur as lenticular masses within diamond-bearing gneiss and marble, and yield P-T estimates of $P > 6$ GPa and $T = 950–1050°C$ based on coesite exsolution from titanite in marble (Ogasawara et al., 2002), K_2O content in clinopyroxene, and garnet-clinopyroxene geothermometry (Okamoto et al., 2000; Katayama et al., 2002) (Fig. 1). Metamorphic diamonds have been identified in pelitic gneisses, marbles, and garnet pyroxenites from the Kumdy-Kol region in the central part of the massif (Sobolev and Shatsky, 1990; Zhang et al., 1997; Ogasawara et al., 2000; Katayama et al., 2000b, 2001). Coesite also widely occurs in eclogite, mica schist, and whiteschist as inclusions in zircon and garnet from the Kumdy-Kol, Barchi-Kol, and Kulet regions (e.g., Shatsky et al., 1995; Korsakov et al., 1998; Parkinson, 2000). Ultrahigh-P metamorphism of the diamond-bearing and associated rocks took place in the Middle Cambrian, as indicated by Sm-Nd and U-Pb zircon of ages between 530 and 540 Ma (Cloué-Long et al., 1991; Shatsky et al., 1999). Muscovite and biotite of diamond-bearing gneiss yielded ^{40}Ar-^{39}Ar of ages 517 ± 5 Ma and 516

TABLE 2. Representative Mineral Compositions of Inclusions in Zircon

Mineral	Garnet		Matrix		Clinopyroxene			Phengite	Albite	Epidote	Rutile	Glass	
	Zircon core	Zircon mantle			Zircon core	Matrix core	Matrix rims	Cpx inc.	Comp. inc.	Comp. inc.	Comp. inc.	Zircon core	Comp. inc.
SiO_2	39.02	38.73	39.39		54.66	53.25	55.36	50.31	67.40	38.56	0.05	45.76	36.10
TiO_2	0.11	0.05	0.05		0.32	0.22	0.11	0.02	0.02	0.16	99.03	0.04	0.06
Al_2O_3	21.11	21.22	21.47		10.81	5.52	9.60	22.57	18.73	8.79	0.01	12.82	22.62
Cr_2O_3	0.02	0.02	0.02		0.00	0.02	0.03	0.06	0.00	0.02	0.03	0.00	0.04
FeO	25.52	24.04	23.56		8.42	9.80	8.76	6.56	0.27	17.77	0.31	10.53	15.17
MnO	0.56	0.54	0.50		0.07	0.05	0.08	0.00	0.04	0.64	0.01	0.12	0.22
MgO	6.77	6.93	6.21		7.25	9.94	6.92	4.21	0.03	0.35	0.01	3.95	12.02
CaO	6.97	7.83	8.36		12.59	16.05	11.95	0.22	0.90	31.73	0.01	4.36	0.05
Na_2O	0.02	0.02	0.05		5.91	3.49	6.30	0.08	10.85	0.02	0.01	0.24	0.02
K_2O	0.00	0.01	0.00		0.00	0.23	0.06	9.58	0.02	0.00	0.00	4.89	1.13
Total	100.10	99.38	99.60		100.03	98.57	99.15	0.00	98.24	98.04	99.47	82.71	87.42
O =	12	12	12		6	6	6	11	8				
Si	3.02	3.01	3.04		1.97	1.99	2.02	3.49	3.00				
Ti	0.01	0.00	0.00		0.01	0.01	0.00	0.00	0.00				
Al	1.93	1.94	1.96		0.46	0.24	0.41	1.85	0.98				
Cr	0.00	0.00	0.00		0.00	0.00	0.00	0.01	0.00				
Fe^{3+}	0.03	0.06	0.00		0.00	0.12	0.00	0.00	0.00				
Fe^{2+}	1.62	1.51	1.52		0.25	0.23	0.27	0.38	0.01				
Mn	0.04	0.04	0.03		0.00	0.00	0.00	0.00	0.00				
Mg	0.78	0.80	0.72		0.39	0.55	0.38	0.44	0.00				
Ca	0.58	0.65	0.69		0.49	0.64	0.47	0.02	0.04				
Na	0.00	0.00	0.01		0.41	0.25	0.45	0.01	0.94				
K	0.00	0.00	0.00		0.00	0.01	0.00	0.85	0.00				
Total	8.01	8.01	7.97		3.99	4.04	4.00	7.02	4.98				
Fe	1.65	1.56	1.52		0.25	0.35	0.27	0.38	0.01				
X_{Ca}	0.19	0.22	0.30	CaTs	0.03	0.01	0.00						
Fe/Mg	2.07	1.88	2.11	Acm	0.00	0.12	0.00						
				Jd	0.40	0.11	0.41						
				CaEs	0.06	0.00	0.00						
				Aug	0.43	0.63	0.47						

± 5 Ma, respectively, which have been interpreted as cooling ages (Shatsky et al., 1999). SHRIMP U-Pb dating of UHP mineral-bearing zircon cores and sub-UHP mineral-bearing rims (representing peak UHP and retrograde metamorphism) yield 537 ± 9 and 507 ± 8 Ma, respectively (Katayama et al. 2001), although Hermann et al. (2001) dated that UHP core, HP granulite mantle, and amphibolite-facies rims at 527 ± 5, 528 ± 8, and 526 ± 5 Ma, respectively.

Petrography and Mineral Chemistry

Petrography

Eclogite samples from the Kumdy-Kol region are intercalated within diamond-bearing gneisses and marbles. Detailed petrography and mineral chemistry of the Kumdy-Kol eclogites have already been described by Okamoto et al. (2000). The studied eclogite sample (#K06) consists of garnet + clinopyroxene + quartz + rutile (Table 1). Symplectite (augite + albite with minor ilmenite) is dominant in matrix clinopyroxene. Garnet contains few inclusion minerals. In garnet aggregate domains, K-rich clinopyroxenes (K_2O = 0.24 wt%) are preserved (Table 2). In these clinopyroxenes, phengites are preserved in the core and secondary K-feldspar in the rim.

More than 500 zircon grains were separated from the eclogite sample (#K06). Approximately 200 zircon grains were mounted on an epoxy disc and polished. Mineral inclusions from 78 zircons were examined. Most zircons are rounded and colorless, and are less than 100 microns in size. Secondary electron microscope images revealed that many zircons show distinct, and typically complex zonal features. The zoning pattern is also confirmed by cathodoluminescent (CL) colors. Backscattered electron images of zoned zircons are shown in Figures 2 and 3. They consist of a dark core (brightest in CL), a lighter mantle, and a rim. A metamict zone the center of the core. The core-mantle boundaries are generally very sharp.

Analytical techniques

Chemical analysis of major elements was performed using an electron probe microanalyzer (JEOL-JXA8800; Jeol Co. Ltd, Tokyo, Japan). All analyses were performed at an accelerating voltage of 15 kV, 12 nA beam current, and counting time of 10-20 s. The oxide, atomic number, absorption and fluorescence (ZAF) correction was employed. The

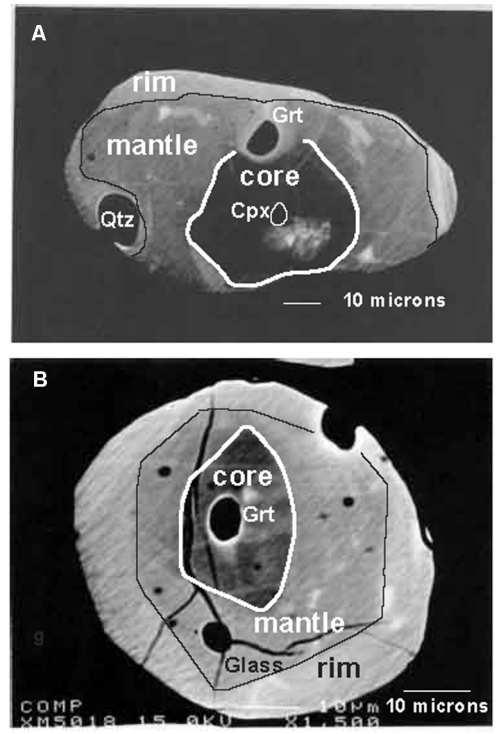

FIG. 2. BSE image of representative zircon zonal texture. The dark core has an idiomorphic outline, and contains a luminescent metamict zone. The relatively brighter mantle is rimmed by a brightest thin zone.

Fe^{3+} contents and CaEs ($Ca_{0.5}\,\square_{0.5}AlSi_2O_6$) component in clinopyroxene were calculated based on the work of Ryburn et al. (1976) and Katayama et al. (2000a), respectively. Calculation details were also described in Okamoto et al. (2000).

Inclusions in zircon

The distribution of inclusions shows a correlation with the zonal texture of the host zircon (Table 1). The core contains garnet, clinopyroxene, and glass, whereas garnet, rutile, and composite inclusions (multiple inclusions) occur in zircon mantles. Chemical composition of the glass is variable and inaccurate because the domain was less than three microns across. Analytical data suggest that this material was K- and Ca-rich fluid or melt (Table 2). The composite inclusions consist of multiple inclusions within a single rounded domain (Fig. 3). Thus textural characteristics indicate that zircon cores grew at the peak UHP stage (or early retrograde

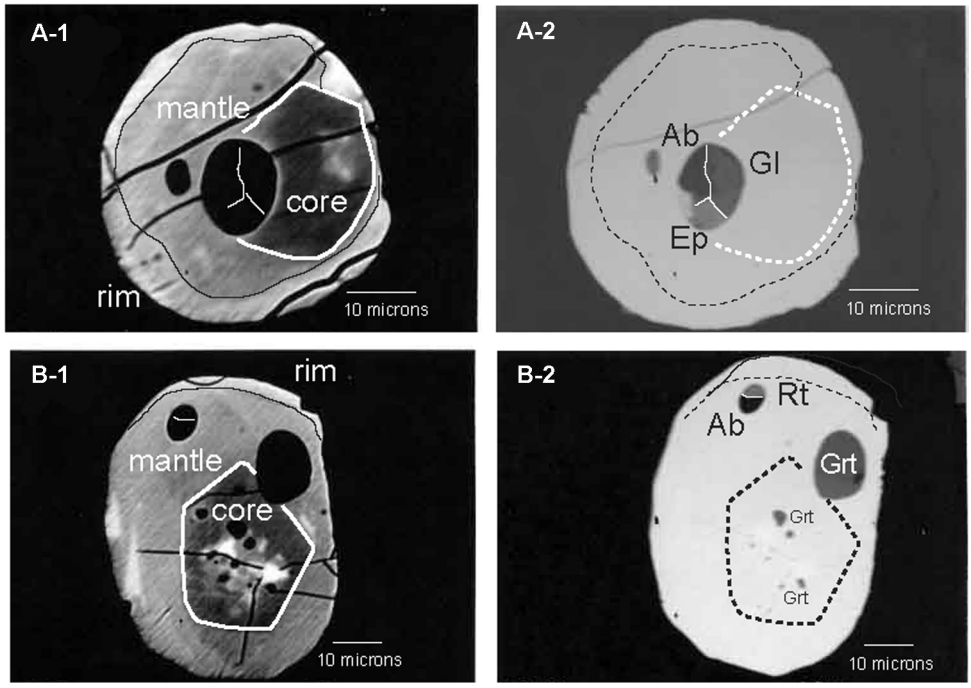

FIG. 3. BSE image of composite inclusions in zircons. Zircons (A and B) exhibit high contrast (A-1, and B-1) and low contrast (A-2 and B-2), respectively. A-1 and B-1 show zonal structure of the zircons, and A-2 and B-2 show composite and single inclusions. Abbreviations: Grt = garnet; Rt = rutile; Gl = glass; Ep = epidote; Ab = albite. In A-2, three inclusions have triple junction boundaries in a single rounded domain. Zircon grew from the domain wall to the interior. In B-2, two-phase composite inclusions have a sharp boundary.

stage?) after phengite was consumed, whereas the rims grew in the quartz stability field during decompression.

The composite inclusions have assemblages of albite + epidote + glass, rutile + ilmenite, quartz + rutile, and rutile + albite (Table 1). The three-phase composite inclusions (albite + epidote + K-bearing glass) (Table 2) have rounded outlines and triple-junction grain boundaries. Zircon overgrew from the wall to interior of the composite domain (Fig. 3A-2). Two-phase inclusions are characterized by a combination with rutile, namely rutile with garnet, albite, quartz, or ilmenite.

The chemistry of garnet and clinopyroxene inclusions also support the idea that zircon cores grew at the UHP stage and rims at the decompression stage. Garnet from the cores contains higher almandine + spessartine components and lower grossular component than that of rims and matrix (Fig. 4A). Clinopyroxene from the core has higher jadeite component than that from the matrix (Fig. 4B). As described above, clinopyroxenes are absent from the mantle and rim of the zircons. Clinopyroxene inclusions in zircon contains a significant (maximum = 11 mol% and average = 4 mol%) (Table 2) CaEs component ($Ca_{0.5}\square_{0.5}AlSi_2O_6$), although this component is negligible in the matrix clinopyroxene. This is consistent with clinopyroxene compositions of coesite-bearing eclogite samples from the Kumdy-Kol area (Katayama et al., 2000a).

Discussion and Conclusion

The relation between zonation and inclusion mineralogy from zircon suggests that phengite was consumed when the zircon core formed. As mentioned above, the three-phase composite inclusions of albite + glass + epidote have rounded outlines and triple-junction grain boundaries. The zircon overgrew from wall to interior of the composite

domain. These features suggest that the composite inclusions may have crystallized from a fluid or melt phase during late UHP or retrograde phengite decomposition. Mineral assemblages in zircon cores and mantles delineate a phengite-consuming reaction: phengite + clinopyroxene (+ coesite) = garnet + rutile + fluid/melt. A similar reaction such as phengite + clinopyroxene + coesite = melt + garnet has been investigated in several UHP experiments (e.g., Schmidt, 1996; Okamoto and Maruyama, 1998).

We compared the chemical compositions of the glass with fluid/melt trapped in UHP and kimberlitic diamonds, and experimentally determined melts from basalt. In Figure 5, single glass inclusions in the zircons are K-rich and Na-poor. On the other hand, melt compositions from hydrous K-rich MORB (and even metasediments) experiments at 4–5 GPa are K-rich and Ca-poor (Schmidt et al., 2004). The melts derived from basaltic compositions at 1–2.5 GPa, are Na-rich and identical with TTG and adakites (e.g., Martin, 1999). This suggests that the glass formed at UHP peak or early retrograde conditions.

Schmidt et al. (2004) have recently re-determined the phengite-out reaction above 6.5 GPa. They suggested that a supercritical melt containing potassium and other solutes appears at pressure above a singular endpoint (or second critical point) (Ricci, 1951; Boettcher and Wyllie, 1969; Stalder et al., 2000; Poli and Fumagalli, 2003). At pressures above the second critical point, there is complete miscibility between melt and fluid. Such a melt/fluid phase is termed "supercritical melt," which increases element solubility continuously from low T to high T. The lack of matrix phengite in the Kumdy-Kol eclogite (Okamoto et al., 2000) suggests that phengite decomposed during prograde UHP metamorphism at P > 6 GPa, supporting the interpretation by Schmidt et al. (2004). Moreover, systematic change in bulk geochemistry of Kokchetav mafic rocks from amphibolite to diamond-grade eclogite also supports K-dissolution due to phengite decomposition at the UHP stage. Concentrations of K and other LIL elements decrease with increasing metamorphic grade, whereas no variation in HFS elements occurs with increasing metamorphic grade (Yamamoto et al., 2002).

The existence of two-phase composite inclusions (rutile with quartz or albite) implies that the "supercritical" melt phase was Si-rich and heterogeneous. Presence of rutile in the two-phase composite indicates that rutile was insoluble in the supercritical melt. That is, even where pressure exceeded the second critical point, HFS elements are retained in rutile from both subducting and exhuming oceanic crust.

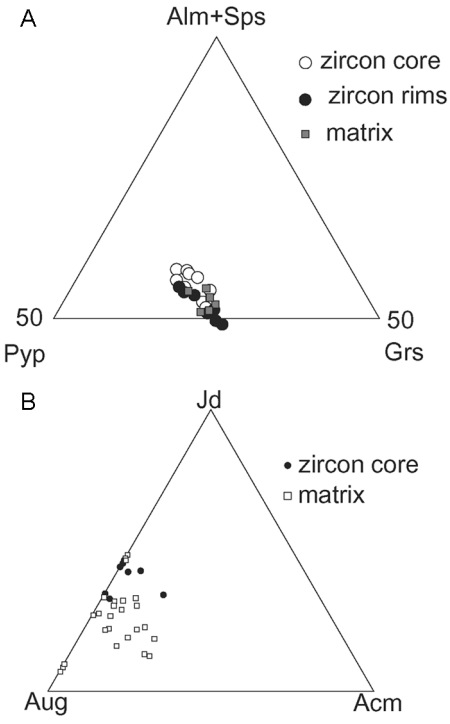

FIG. 4. Garnet (A) and clinopyroxene (B) compositions from the zircon inclusions and matrix. Abbreviations: Alm = almandine; Sps = spessartine; Grs = grossular; Jd = jadeite; Aug = augite; Acm = acmite.

The present study concludes that the subducted Kokchetav UHP eclogites lacked fluid- and K-bearing phases at depths of approximately 180 km. However, minor fossil fluids may have been preserved in zircon as well as in clinopyroxene (Katayama and Nakashima, 2003), garnet and rutile (Katayama et al., 2006).

Acknowledgments

We thank Drs. Lin-gun Liu and Tzen-Fu Yui for discussions, Dr. Yoshi Iizuka for EPMA analysis, and Dr. Tzen-Fu Yui for manuscript review. Preparation of the manuscript was supported in part by NSF EAR-0506901.

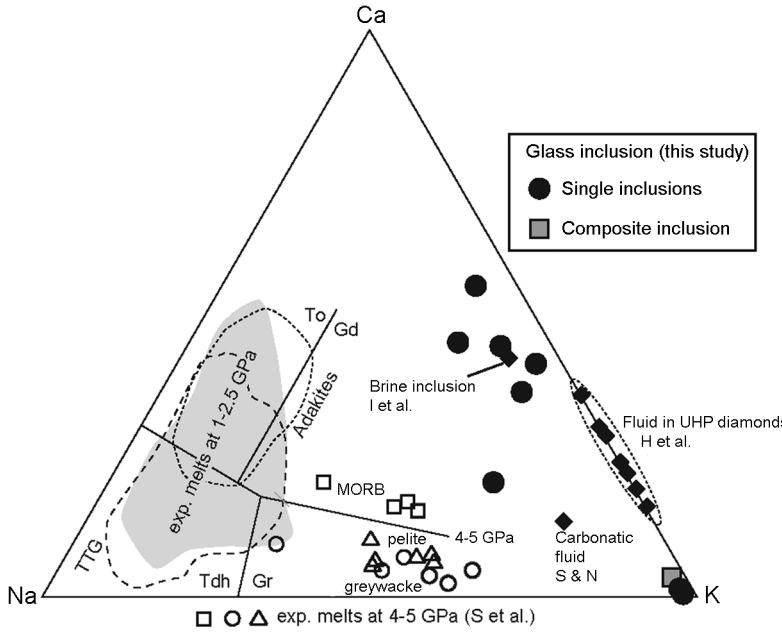

FIG. 5. Melt and fluid compositions under UHP conditions. The present study shows that fluid compositions (glass) are relatively Na-poor and K-rich. The compositions are comparable with fluid inclusions in UHP diamonds (H et al. = Hwang et al, 2005) and in kimberlite diamonds (S & N = Schrauder and Navon, 1994; I et al. = Izraeli et al., 2001). Experimentally determined melt composition from basalts at 1–2.5 GPa (grey field) are from Schmid et al. (2004) (original fields are from Martin, 1999). Melt compositions at 4-5 GPa (from S et al. = Schmidt et al., 2004) are relatively Ca-poor and K-rich. Abbreviations: To = tonalite; Gd = granodiorite; Tdh = trondhjemite; Gr = granite; TTG = tonalite-trondhjemite-granite.

REFERENCES

Akaogi, M., Kusaba, K., Susaki, J-I., Yagi, T., Matsui, M., Kikegawa, T., Yusa, H., and Ito, E., 1992, High-pressure high-temperature stability of αPbO_2-type TiO_2 and $MgSiO_3$ majorite: Calorimetric and in situ X-ray diffraction studies, *in* Syono, Y., and Manghani, M. H., eds., High pressure research: Applications to Earth and Planetary Sciences: Washington, DC, American Geophysical Union, p. 447–455.

Bohlen, S. R., and Boettcher, A. L., 1982, The quartz-coesite transformation: A precise determination and the effects of other components: Journal of Geophysical Research, v. 87, p. 7073–7078.

Boettcher, A. L., and Wyllie, P. J., 1969, The system $CaO-SiO_2-CO_2-H_2O$—III. Second critical end-point on the melting curve: Geochimica Cosmochimica Acta, v. 33, p. 611–632.

Bundy, F. R., 1980, The P, T phase reaction diagrams for elemental carbon: Journal of Geophysical Research, v. 85, p. 6930–6936.

Chopin, C, and Sobolev, N. V., 1995, Principal mineralogic indicators of UHP in crustal rocks, *in* Coleman, R. G., and Wang, X. eds., Ultrahigh-pressure metamorphism: Cambridge, UK, Cambridge University Press, p. 96–131.

Cloué-Long, J. C., Sobolev, N. V., Shatsky, V. S., and Sobolev, A. V., 1991, Zircon response to diamond pressure metamorphism in the Kokchetav massif, USSR: Geology, v. 19, p. 710–713.

Dobretsov, N. L., Sobolev, V. S., Shatsky, V. S., Coleman, R. G., and Ernst, W. G., 1995, Geotectonic evolution of diamondiferous paragneisses, Kokchetav Complex, northern Kazakhstan: The geologic enigma of ultrahigh-pressure crustal rocks within a Paleozoic fold belt: The Island Arc, v. 4, p. 267–279.

Hermann, J., Rubatto, D., Korsakov, A., and Shatsky, V., 2001, Multiple zircon growth during fast exhumation of diamondiferous, deeply subducted continental crust (Kokchetav Massif, Kazakhstan): Contributions to Mineralogy and Petrology, v. 141, p. 66–82.

Hwang, S.-L., Shen, P., Chu, H.-T., Yui, T.-F., Liou, J. G., Sobolev, N. V., and Shatsky, V. S., 2005, Crust-derived

potassic fluid in metamorphic microdiamond: Earth and Planetary Science Letters, v. 231, p. 295–306.

Izraeli, E. S., Harris, J. W., and Navon, O., 2001, Brine inclusions in diamonds: A new upper mantle fluid: Earth and Planetary Science Letters, v. 187, p. 323–332.

Kaneko, Y., Maruyama, S., Terabayashi, M., Yamamoto, H., Ishikawa, M., Anma, R., Parkinson, C. D., Ohta, T., Nakajima, Y., Katayama, I., Yamamoto, J., and Yamauchi, K., 2000, Geology of the Kokchetav UHP-HP metamorphic belt, northern Kazakhstan: The Island Arc, v. 9, p. 264–283.

Katayama, I., Maruyama, S., Parkinson, C. D., Terada, K., and Sano, Y., 2001, Ion micro-probe U-Pb zircon geochronology of peak and retrograde stages of ultrahigh-pressure metamorphic rocks from the Kokchetav massif, northern Kazakhstan: Earth and Planetary Science Letters, v. 188, p. 185–198.

Katayama, I., and Nakashima, S., 2003, Hydroxyl in clinopyroxene from the deep subducted crust: Evidence for H_2O transport into the mantle: American Mineralogist, v. 88, p. 229–234.

Katayama, I., Nakashima, S., and Yurimoto, H., 2006, Water content in natural eclogite and implication for water transport into the deep upper mantle: Lithos, v. 86, p. 245–259.

Katayama, I., Ohta, M., and Ogasawara, Y., 2002, Mineral inclusions in zircon from diamond-bearing marble in the Kokchetav massif, northern Kazakhstan: European Journal of Mineralogy, v. 14, p. 1103–1108.

Katayama, I., Parkinson, C. D., Okamoto, K., Nakajima, Y., and Maruyama, S., 2000a, Supersilicic clinopyroxene and silica exsolution in UHPM eclogite and pelitic gneiss from the Kokchetav massif, Kazakhstan: American Mineralogist, v. 85, p. 1368–1374.

Katayama, I., Zayachkovsky, A. A., and Maruyama, S., 2000b, Prograde pressure-temperature records from inclusions in zircons from ultrahigh-pressure-high-pressure rocks of the Kokchetav Massif, northern Kazakhstan: The Island Arc, v. 9, p. 417–427.

Korsakov, A. V., Shatsky, V. S., and Sobolev, N. V., 1998, The first finding of coesite in the eclogites of the Kokchetav massif: Doklady, Earth Science Series, v. 360, p. 469–473.

Martin, H., 1999, Adakitic magmas: Modern analogues of Archean granitoids: Lithos, v. 46, p. 411–429.

Maruyama, S., Liou, J. G., and Terabayashi, M., 1996, Blueschists and eclogites of the world and their exhumation: International Geology Review, v. 38, p. 485–594.

Ogasawara, Y., Fukasawa, K., and Maruyama, S., 2002, Coesite exsolution from titanite in UHP marble from the Kokchetav Massif: American Mineralogist, v. 87, p. 452–461.

Ogasawara, Y., Ohta, M., Fukasawa, K., Katayama, I., and Maruyama, S., 2000, Diamond-bearing and diamond-free metacarbonate rocks from Kumdy-Kol in the Kokchetav Massif, northern Kazakhstan: The Island Arc, v. 9, p. 400–416.

Okamoto, K., Liou, J. G., and Ogasawara, Y., 2000, Petrology of the diamond-grade eclogite in the Kokchetav Massif, northern Kazakhstan: The Island Arc, v. 9, p. 379–399.

Okamoto, K., and Maruyama, S., 1998, Multi-anvil re-equilibration experiments of a Dabie Shan ultrahigh-pressure eclogite within the diamond-stability fields: The Island Arc, v. 7, p. 52–69.

Okamoto, K., and Maruyama, S., 1999, The high pressure stability limits of lawsonite in the MORB + H_2O system: American Mineralogist, v. 84, p. 362–373.

Parkinson, C. D., 2000, Coesite inclusions and prograde compositional zonation of garnets in whiteschists of the Kokchetav UHP-HP massif, Kazakhstan: A unique record of progressive UHP metamorphism: Lithos, v. 52, p. 215–233.

Peacock, S. M., and Wang, K., 1999, Seismic consequences of warm versus cool subduction metamorphism: Examples from southwest and northeast Japan: Science, v. 286, p. 937–939.

Poli, S., and Fumagalli, P., 2003, Mineral assemblages in ultrahigh pressure metamorphism: A review of experimentally determined phase diagrams, *in* Carswell, D. A., and Compagnoni, R., eds., Ultrahigh-pressure metamorphism: Budapest, Hungary, Eötvös University Press, p. 307–340.

Poli, S., and Schmidt, M. W., 1995, H_2O transport and release in subduction zones: Experimental constraints on basaltic and andesitic systems: Journal of Geophysical Research, v. 100, p. 22,299–22,314.

Ricci, J. E., 1951, The phase rule and heterogeneous equilibrium: New York, NY, Dover Publications, 505 p.

Ryburn, R. J. R., Råheim, A., and Green, D. H., 1976, Determination of the P, T paths of natural eclogites during metamorphism-record of subduction: A correction to a paper by Råheim and Green (1975): Lithos, v. 9, p. 161–164.

Schmidt, M. W., 1996, Experimental constraints on recycling of potassium from subducted oceanic crust: Science, v. 272, p. 1927–1930.

Schmidt, M. W., and Poli, S., 1998, Experimentally based water budgets for dehydrating slabs and consequences for arc magma generation: Earth and Planetary Science Letters, v. 163, p. 361–379.

Schmidt, M. W., Vielzeuf, D., and Auzanneau, E., 2004, Melting and dissolution of subducting crust at high pressures: The key role of white mica: Earth and Planetary Science Letters, v. 228, p. 65–84.

Schrauder, M., and Navon, O., 1994, Hydrous and carbonatitic mantle fluids in fibrous diamonds from Jwaneng, Botswana: Goechimica et Cosmochimica Acta, v. 58, p. 761–771.

Shatsky, V. S., Sobolev, N. V., and Vavilov, M. A., 1995, Diamond-bearing metamorphic rocks of the Kokchetav

Massif (northern Kazakhstan), in Coleman, R. G., and Wang, X ., eds., Ultrahigh-pressure metamorphism: Cambridge, UK, Cambridge University Press, p. 427–455.

Shatsky, V. S., Jagoutz, E., Sobolev, N. V., Kozmenko, O. A., Parkhomento, V. S., and Troesch, M., 1999, Geochemistry and age of ultra-high pressure rocks from the Kokchetav massif, northern Kazakhstan: Contributions to Mineralogy and Petrology, v. 137, p. 185–205.

Sobolev, N. V., and Shatsky, V. S., 1990, Diamond inclusions in garnets from metamorphic rocks: Nature, v. 343, p. 742–746.

Stalder, R., Ulmer, P., Thompson, A. B., and Gunter, D., 2000, Experimental approach to constrain second critical end points in fluid/silicate systems: Near-solidus fluids and melts in the system albite-H_2O: American Mineralogist, v. 85, p. 68–77.

Tatsumi, Y., and Eggins, S., 1995, Subduction zone magmatism: Oxford, UK, Blackwell, Frontiers in Earth Sciences, 211 p.

Tatsumi, Y., Hamilton, D. L., and Nesbit, R. W., 1986, Chemical characteristics of fluid phase from a subducted lithosphere and origin of arc magmas: Evidence from high-pressure experiments and natural rocks: Journal of Volcanology and Geothermal Research, v. 29, p. 293–309.

Usui, T., Nakamura, E., Kobayashi, K., Maruyama, S., and Helmstaedt, H., 2003, Fate of the subducted Farallon plate inferred from eclogite xenoliths in the Colorado Plateau: Geology, v. 31, p. 589–592.

Withers, A. C., Essene, E. J., and Zhang, Y., 2003, Rutile/TiO_2 II phase equilibria: Contributions to Mineralogy and Petrology, v. 145, p. 199–204.

Yamamoto, J., Maruyama, S., Parkinson, C. D., and Katayama, I., 2002, Geochemical characteristics of metabasites from the Kokchetav Massif: Subduction zone metasomatism along an intermediate geotherm, in Parkinson, C. D. et al., eds., The diamond-bearing Kokchetav Massif, Kazakhstan: Tokyo, Japan, University Academy Press, Frontier Science Series no. 38, p. 363–372.

Zhang, R. Y., Liou, J. G., Ernst, W. G., Coleman, R. G., Sobolev, N. V., and Shatsky, V. S., 1997, Metamorphic evolution of diamond-bearing and associated rocks from the Kokchetav Massif, northern Kazakhstan: Journal of Metamorphic Geology, v. 15, p. 479–496.